IJLAI Transactions on Science and Engineering (ISSN: 3006-3418) 2025, vol. 3, no. 2, pp: 11–15

Analysis of Static Characteristics and Optimization of Basic Parameters of Static Pressure Gas Bearings for Precision Machine Tools

Xi Zhang[1]

1. School of Mechanical Engineering, Zhengzhou University of Science and Technology
Zhengzhou, 450064 China
zhangxi_9534@163.com
Received April. 15, 2025; Revised and Accepted May. 16, 2025

Abstract. This paper conducts research on the hydrostatic gas bearings of precision machine tools, deeply analyzes their static characteristics and optimizes the basic parameters. Firstly, through theoretical modeling, the static characteristic equation of the hydrostatic gas bearing was derived, covering key indicators such as stiffness and bearing capacity. Subsequently, combined with the numerical simulation method, the static characteristic performance of the bearing under different working conditions was simulated to verify the accuracy of the theoretical model. The research finds that the static characteristics of gas bearings are significantly affected by parameters such as gas supply pressure and bearing clearance. Based on this, the basic parameters of the bearing were optimized and designed by using the optimization algorithm, and the optimal parameter combination was determined, which significantly improved the load-bearing capacity and stiffness of the bearing while reducing power consumption. The experimental results show that the application of the optimized hydrostatic gas bearing in precision machine tools can significantly improve the processing accuracy and stability, providing a theoretical basis and technical support for the design of high-performance bearings in high-end precision machine tools, and has important engineering application value.

Keywords: Precision machine tools, Ultra-precision, Gas bearings, Static characteristics.

1. Introduction

Gas-lubricated bearings generally use air as the bearing lubricant, and thus are often also referred to as air-lubricated bearings. Gas-lubricated bearing technology is a high-tech that developed rapidly in the middle of the 20th century. Compared with traditional bearing technology, it has many excellent characteristics, such as extremely low friction, small temperature rise, no pollution, no wear, high rotational accuracy, and the ability to work well in harsh environments [1,2].

Hydrostatic gas bearings have high rotational accuracy at high speeds. When applied to the main shaft support of precision machinery, they can achieve high processing accuracy. In the development history of precision and ultra-precision machine tools at home and abroad, many very typical precision and ultra-precision machine tools have emerged, and their spindle systems all adopt gas bearings. For example, the hemispherical lathe produced by the Union Carbide Corporation of the United States can process hemispheres of 4100mm. The dimensional accuracy of the parts can reach $\pm 0.6\mu m$, and the surface roughness can reach $0.025\mu m$. This is the earliest ultra-precision machine tool that combines gas-lubricated bearings with diamond tools. The OAGM2500 large ultra-precision machine tool developed by Cranfield University Precision Engineering Company (CUPE) in the UK features a grinding head and a measuring head supported by gas-lubricated bearings, which can achieve high rotational accuracy [3-5]. It is mainly used for grinding large curved surface mirrors of X-ray astrotelescopes and can also be applied in ultra-precision turning and coordinate measurement. Its resolution can reach 2.5nm. The ultra-high-speed spindle developed by Luoyang Bearing Research Institute in China is supported by gas-lubricated floating ring hydrostatic and hydrodynamic hybrid bearings. The spindle speed can reach $3.0 \times 10r/min$. It is used for grinding the inner surface of small holes ranging from 41mm to 3mm, and its surface roughness can reach $0.2\mu m$. Moreover, this type of spindle has low power consumption and a long working life.

2. Theoretical Analysis of the Static Characteristics of Hydrostatic Gas Bearings

As shown in Figure 1, the small-hole throttling radial hydrostatic gas bearing for the spindle of the machine tool in this experiment has a total length of L and a shaft diameter of D. The gas film gap h between the shaft and the shaft sleeve is much smaller than the diameter D, so it can be approximately considered that the inner diameter of the hydrostatic gas bearing is also D. The hydrostatic gas bearing has an air inlet and a throttling hole, which are

evenly distributed circumferentially on the end face at a distance of l from the shaft end. Each air inlet has a small hole throttling device. Under the action of the self-weight of the bearing and the load, the rotor and the bearing become eccentric [6,7]. Due to the compressibility of the gas, a pressure difference can be generated at the place where the gas film gap is the smallest and the place where the gap is the largest. The resultant force is balanced with the load, that is, the load-bearing capacity is produced, and thus the main shaft can be lifted during operation.

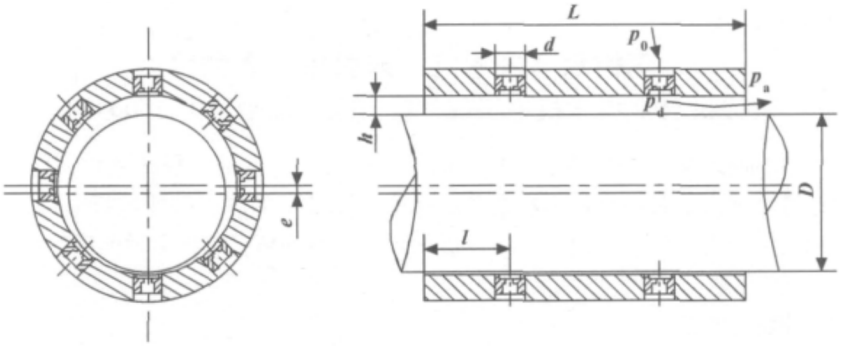

Fig. 1. Structural diagram of small hole throttling hydrostatic gas bearing

Assuming the flow of gas is an isothermal process and considering the compressibility of gas, when the shaft and the shaft sleeve are relatively stationary, the pressure p at each point within the gas film of the hydrostatic gas bearing should satisfy the Reynolds equation.

$$\frac{\partial}{\partial x}(\frac{\partial p^2}{\partial x}) + \frac{\partial}{\partial z}(\frac{\partial p^2}{\partial z}) + Q\delta_i = 0. \tag{1}$$

In the formula, p represents the gas supply pressure. h is the clearance of the bearing. Q represents the flow rate. δ_i is the flow factor (taking the value of 0 where there is no throttle hole and 1 where there is a throttle hole).

To solve equation (1), the finite element method is adopted to discretize the Reynolds equation. Meanwhile, let $\bar{f} = f(x, z)$ represents the square value of the pressure of the hydrostatic gas bearing, which is simply referred to as the pressure square function or pressure square. If $f(x, z)$ is regarded as the independent variable, a functional can be formed [8].

$$\Phi(f(x,z)) = \int_{\Omega} \frac{\bar{h}^3}{2}[(\frac{\partial \bar{f}}{\partial \bar{x}})^2 + (\frac{\partial \bar{f}}{\partial \bar{z}})^2] - Qf(x,z)\delta_i d\bar{x}d\bar{z}. \tag{2}$$

It can be known from equation (2) that $\Phi(f)$ varies with the change of the pressure function $f(x, z)$. Therefore, it is a functional with the pressure function as the independent variable, that is, each different pressure distribution corresponds to a related functional value. Therefore, the squared function $f(x, z)$ that can make the functional $\Phi(f)$ take extreme values is the solution of the Reynolds equation (1). To solve the extreme values of Equation (2), the finite element method is employed. The integration over the entire 2-field is changed to the integration over each finite element, and then the sum is obtained as follows:

$$\Phi(f) = 0.5\sum_{\lambda=1}^{n}\int_{\Delta\lambda} \bar{h}^3[(\frac{\partial \bar{f}}{\partial \bar{x}})^2 + (\frac{\partial \bar{f}}{\partial \bar{z}})^2] - \sum_{\lambda=1}^{n} Qf(x,z)\delta_i d\bar{x}d\bar{z}. \tag{3}$$

By differentiating equation (3) and setting its value to 0, the relationship of the node squared function where $\Phi(f)$ is an extreme value can be obtained. Then, by using the super-relaxation iterative method and the proportional division method to obtain the solution of the pressure square function relationship, the pressure square values of each node on the surface of the small-hole throttling hydrostatic gas bearing can be obtained.

2.1. Calculation of the Load-bearing Capacity of Hydrostatic Gas Bearings

After solving the pressure equation system, the node pressure square distribution of the small-hole throttling hydrostatic gas bearing can be obtained [9,10]. Then, the load-bearing capacity of each element can be determined, and further, the total load-bearing capacity W of the small-hole throttling hydrostatic gas bearing can be calculated.

$$W = \sum_{\lambda=1}^{n} W_{\lambda}. \tag{4}$$

Where W represents the total load-bearing capacity of the hydrostatic gas bearing. W_{λ} represents the bearing capacity of each finite unit. λ represents the number of finite element bodies.

2.2. Calculation of the Stiffness of Hydrostatic Gas Bearings

The direction of action of the total load-bearing capacity of the hydrostatic gas bearing is opposite to the direction of change of eccentricity. After obtaining the load-carrying capacity of the bearing under different eccentricities, the stiffness of the hydrostatic gas bearing can be derived from the following formula.

$$K_J = \frac{\Delta W}{\Delta e}. \tag{5}$$

2.3. Calculation of Gas Supply Volume for Hydrostatic Gas Bearings

The gas supply volume of a hydrostatic gas bearing is the sum of the flow rates of each throttle hole. For a hydrostatic gas bearing with double rows of throttle holes [11,12], it is calculated by the following formula.

$$M_J = 2\sum_{i=1}^{N} m_r = 2\phi A p_0 \sqrt{\frac{2\rho_a}{p_a}}\varphi. \tag{6}$$

In the formula, A represents the area of the throttle hole. p_0 represents the gas supply pressure at the small hole inlet. p_a represents atmospheric pressure. ρ_a represents the gas density at atmospheric pressure. ϕ is the flow coefficient, which is generally taken as 0.8. φ is the flow function.

3. Optimization of Basic Parameters of Hydrostatic Gas Bearings for Precision Machine Tools

To maximize the stiffness of the bearing and reduce the influence of gas diffusion and circulation on the bearing, the length-to-diameter ratio L/D of the bearing is generally taken as 1, and the position of the throttle hole is $l/L = 1/4$. Combined with the actual situation of the test machine tool in this paper, the main parameters of the front and rear small hole throttling hydrostatic gas bearings for the spindle are selected as follows: $D_1 = 80mm$, $D_2 = 100mm$. The lengths of the front and rear bearings are respectively: $L_1 = 80mm$, $L_2 = 100mm$. The distance between the throttle hole and the end face of the bearing is $l_1 = 20mm$ and $l_2 = 25mm$. The number of throttle holes $n = 8$. Based on these given parameters, the numerical analysis and calculation of the hydrostatic gas bearing are carried out simultaneously by using the finite element method. Finally, the gas supply pressure p_0, the diameter d_0 of the throttle hole and the average bearing clearance h_0 of the hydrostatic gas bearing are determined.

3.1. Gas Film Pressure Distribution of Small-hole Throttling Hydrostatic Gas Bearings

The length of the static pressure gas bearing in this experiment is $L_1 = 80mm$ with double rows of throttle holes for gas supply. The number of throttle holes is $n = 8$, and the diameter of the static pressure gas bearing is $D_1 = 80mm$. For the convenience of the test analysis, referring to relevant materials, the average clearance h_0 of the static pressure gas bearing in this test is first determined as $20\mu m$, and the diameter of the throttling hole d_0 is determined as 0.2mm.

The mathematical model for solving the finite element of the static pressure gas bearing was utilized, and the parameters were numerically calculated by programming with Matlab software to obtain the gas film pressure distribution of the small hole throttling static pressure gas bearing. The outlet pressure values of the 8 throttle holes are the local maximum values. The smaller the thickness of the gas film at the location of the throttle holes, the greater the outlet pressure of the throttle holes. This is because the thinner the gas film, the greater the gas resistance of the gas film, the smaller the pressure drop generated by the gas flowing through the throttling, and thus the greater the outlet pressure of the throttling hole [13-15].

3.2. Influence of Eccentricity on Load-bearing Capacity and Stiffness Under Different Gas Supply Pressures

At present, the static pressure gas bearing in front of the main shaft is taken as the main research object. The length of the static pressure gas bearing $L_1 = 80mm$, with double rows of throttling holes for gas supply, the number of throttling holes $n = 8$, and the diameter of the static pressure gas bearing $D_1 = 80mm$. Given that the average clearance h_0 of the hydrostatic gas bearing is $20\mu m$ and the throttling hole diameter d_0 is 0.2mm, the relationship curves between the eccentricity ε of the hydrostatic gas bearing and the bearing's load-carrying capacity and stiffness under different gas supply pressures p_0 can be obtained, as shown in figures 2 and 3.

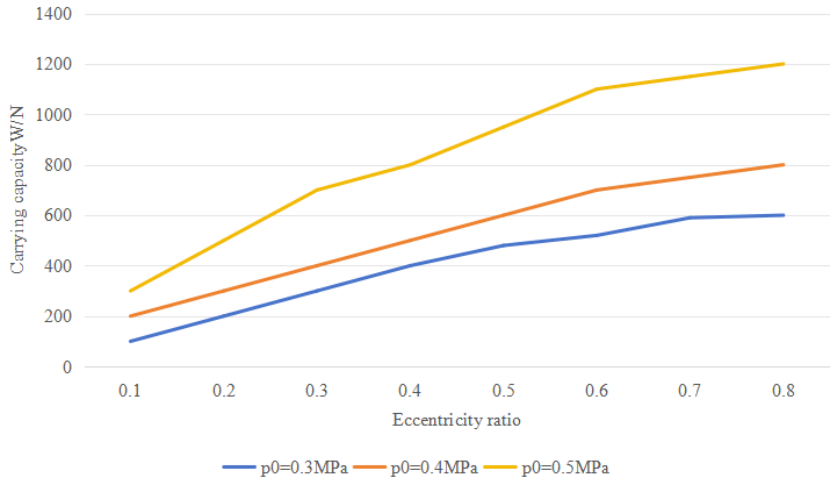

Fig. 2. The relationship curve between eccentricity and bearing capacity under different gas supply pressures

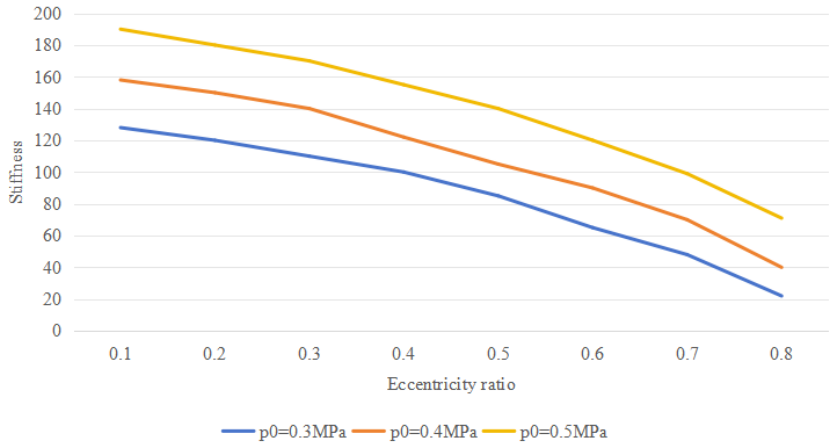

Fig. 3. The relationship curve between eccentricity and stiffness under different gas supply pressures

It can be known that the greater the gas supply pressure is, the greater the load-bearing capacity and stiffness of the hydrostatic gas bearing will be. Under the same gas supply pressure, the bearing capacity increases with the increase of eccentricity, while the stiffness decreases with the increase of eccentricity. Therefore, the eccentricity should have an appropriate range. Both too large and too small eccentricity are not conducive to the normal operation of hydrostatic gas bearings.

4. Conclusion

The Reynolds equation is discretized by the finite element method to solve the static characteristics of the hydrostatic gas bearings of precision machine tools. The relationship between the basic parameters, stiffness and

load-bearing capacity of the hydrostatic gas bearings is analyzed. The basic parameters of the hydrostatic gas bearings at the front and rear of the spindle of the precision machine tool are optimized, and the optimized structural parameters and operating parameters are obtained.

5. Conflict of Interest

The authors declare that there are no conflict of interests, we do not have any possible conflicts of interest.

Acknowledgments. None.

References

1. Luo J, Cao Y, Jin J, et al. Study on the rotation accuracy of gas hydrostatic bearings based on skin model shapes[J]. Precision Engineering, 2025, 94: 435-446.
2. Boyao D, Jianbo Z. The research on the steady characteristics of aerostatic thrust bearing for machine tool spindles with different parameters[J]. Manufacturing Technology & Machine Tool, 2024 (2): 18-23.
3. Zhang K, Zhang X, Zhang R. Study of the Static Characteristics of Gas-Lubricated Thrust Bearings Using Analytical and Finite Element Methods[J]. Applied Sciences, 2024, 14(8): 3459.
4. Zhang G, Huang M, Chen G, et al. Design and optimization of fluid lubricated bearings operated with extreme working performancesła comprehensive review[J]. International Journal of Extreme Manufacturing, 2024, 6(2): 022010.
5. Wang P, Li Y, Gao X, et al. Numerical Analysis on the Static Performance of Gas Journal Bearing by Using Finite Element Method[J]. Nanomanufacturing and Metrology, 2024, 7(1): 3.
6. Dai Y, Deng H, Pan G, et al. A Review of Machine Tool Motorized Spindle Variable Pressure Preload Technology Research[J]. Recent Patents on Engineering, 2025, 19(5): E18722121303527.
7. Lin S, Jiang S. Study on Rotor-Bearing Dynamics of an Improved Machine Tool Spindle with Water-Lubricated Hydrostatic Thrust Bearing and Rolling Bearings[J]. Journal of Vibration Engineering & Technologies, 2025, 13(4): 239.
8. Wu Y, Cao L, Tang J, et al. Global sensitivity analysis of design variables for porous hydrostatic gas bearings considering uncertainty[J]. Probabilistic Engineering Mechanics, 2025, 79: 103722.
9. Yu X, Lin Y, Wang P, et al. Analysis of lubrication characteristics of dynamic-static pressure hybrid thrust bearing considering key factors under eccentric loads[J]. Tribology International, 2024, 194: 109471.
10. Miettinen M, Vainio V, Theska R, et al. On the static performance of aerostatic elements[J]. Precision Engineering, 2024, 89: 1-10.
11. Zhang P, Chen Y. Universal accuracy model for three different types of precision bearings with three basic structures under quasi-static conditions[J]. Proceedings of the Institution of Mechanical Engineers, Part C: Journal of Mechanical Engineering Science, 2024, 238(13): 6331-6354.
12. Yuanqi C, Yaping X, Weining L, et al. Effect of Pressure Equalization Groove Structure on Static Characteristics of Aerostatic Bearings[J]. Journal of Applied Fluid Mechanics, 2025, 18(4): 1086-1097.
13. Song W, Li M, Cheng P, et al. CFD-Based Investigation of Static and Dynamic Pressure Effect in Aerostatic Bearings with Annular Grooves at High Speed[J]. Lubricants, 2025, 13(2): 46.
14. Tian B, Zhang X, Xu J, et al. Research on the static and dynamic characteristics of porous air bearings considering annular groove air supply[J]. Journal of Tribology, 2025, 147(6).
15. Qiu S, Ke C, Li K, et al. Nonlinear dynamic analysis of a novel tangentially supplied aerostatic bearing-rotor system: Theory and experiment[J]. Mechanical Systems and Signal Processing, 2025, 224: 112221.

Biography

Xi Zhang graduated from Zhongyuan University of Technology with a master's degree in mechanical engineering in 2015. After graduation, he had been working in the field of vibration and noise control and automation control. Since 2017, he has been a full-time teacher, teaching assistant and lecturer of Zhengzhou University of Science and Technology.